HOW MASSIVE IS THE BLACK HOLE IN M87?

S.K. CHAKRABARTI
Tata Institute Of Fundamental Research
Homi Bhabha Road, Bombay 400005, INDIA

1. INTRODUCTION

Using the Faint Object Spectrograph (FOS) on Hubble Space Telescope (HST), Harms et al. (1994, H94) have recently reported the spectroscopy of central region of the elliptical galaxy M87. Ford et al. 1994 (hereafter F94), using Wide Field Planetary Camera-2 have imaged the region around the nucleus in H_α+[NII] and find an ionized disk with spiral structures of mainly two arms. From the kinematical argument, based on the Doppler shifts of several lines emitted from the disk, and assuming a Keplerian motion of the emitting gas, they conclude that the mass of the disk plus the nucleus: $M_c(R < 18\text{pc}) = (2.4 \pm 0.7) \times 10^9 M_\odot$ and the inclination angle of the disk with the line of sight is $i = (42 \pm 5)^o$. However, if the bright spiral structures are real, and represent shocked region in the disk, we expect that the disk is strongly non-Keplerian and therefore the mass of the black hole must be higher than above estimation.

In the present contribution, we provide a complete description of the velocity field of the ionized disk and compute the shape of typical line profiles expected from various parts of the disk. Our analysis is based on the solution of a non-axisymmetric disk which includes two armed spiral density waves. We find a very good agreement between the theoretical and observed line profiles as regards to the Doppler shifts, line widths and the intensity ratios and estimate the mass of the black hole to be $(4 \pm 0.2) \times 10^9 M_\odot$. Details of this work will be published elsewhere (Chakrabarti, 1995).

In a binary system with a thin accretion disk, the binary companion can induce two armed spiral shocks in the disk (e.g., Matsuda et al. 1987, Spruit 1987, Chakrabarti & Matsuda, 1992). In the case of active galaxies, a passing companion (or a globular cluster or a dwarf galaxy) which is more massive than the disk can induce the same effect.

I. Appenzeller (ed.), Highlights of Astronomy, Vol. 10, 535–538.

https://doi.org/10.1017/S1539299600011977 Published online by Cambridge University Press

2. MODEL EQUATIONS

Below, we concentrate on disk solutions which include only two self-similar spirals. The spiral shock wave solution is described in detail in the literature (Chakrabarti, 1990). The general procedure of obtaining the line emissions from the spiral disk is also presented elsewhere (Chakrabarti & Wiita, 1994) where it was shown that the time variability of the line emissions from the broad line radio galaxies such as ARP 102B and 3C390.3 can be understood well using non-Keplerian disk with spiral shock waves.

In a self-similar disk, the velocity components vary as,

$$u' = x^{-1/2}q_1(\Psi), \quad v' = x^{-1/2}q_2(\Psi), \quad \text{and} \quad a' = x^{-1/2}q_3(\Psi), \qquad (1)$$

where, u', v', and a' are the radial, azimuthal and sound velocities, respectively, $\Psi = \phi' + B \log(x) = constant$ defines the spiral coordinate, x is the radial co-ordinate r' in units of GM/c^2, M being the mass of the central black hole, and $B = \tan\beta$, with β the pitch angle of the spirals. The functional behaviours of $q_i(\Psi)$ are self-consistently determined from the two-and-a-half dimensional Euler equations: all the terms on the equatorial (r', ϕ') plane are kept, whereas hydrostatic equilibrium is assumed in the vertical direction. The equation of state is chosen to be $P = K(x, \psi)\rho^\gamma$, with $\gamma = 1 + 1/n$. For an assumed number of shocks, given the pitch angle β, and any one of the velocity components on the sonic surface (we supply q_{2c}), the entire set of equations can be solved for all the kinematic quantities and the polytropic index n of the disk. In a strictly Keplerian disk, $q_2 = 1$ and $q_1 = 0$ identically everywhere in the disk. The sound speed in a Keplerian disk varies as $a \propto x^{-3/8}$, so q_3 cannot be compared directly with the Keplerian value.

3. FITTING PROCEDURE OF THE HST RESULTS

We fit the line profiles with the theoretical result by supplying B and q_2 at the sonic surface (to obtain the velocity profiles), and the inclination angle i, the inner and outer edges of the emitting regions, x_{in} and x_{out} respectively, the emissivity law $\epsilon(x) \propto x^{-q}$, thermal broadening velocity v_{th} and the mass of the black hole M to obtain the line intensities (Chakrabarti, 1995). From the locations of the HST observations, we obtain x_{in} and x_{out} directly provided the mass of the hole is known. The relative location of the spiral shock is varied untill a good fit is obtained. First, we fit the profiles of Position 4 of HST data (i.e., nucleus) and check if the same set of parameters consistently reproduce the profiles in Positions 1, 2, 5 and 6. The emitted line profiles are found to be very sensitive to the relative orientation of the spiral shocks with respect to the line of sight and the emissivity $\propto x^{-q}$ — a slight variation of q changes the intensity significantly. In Figure 1, we

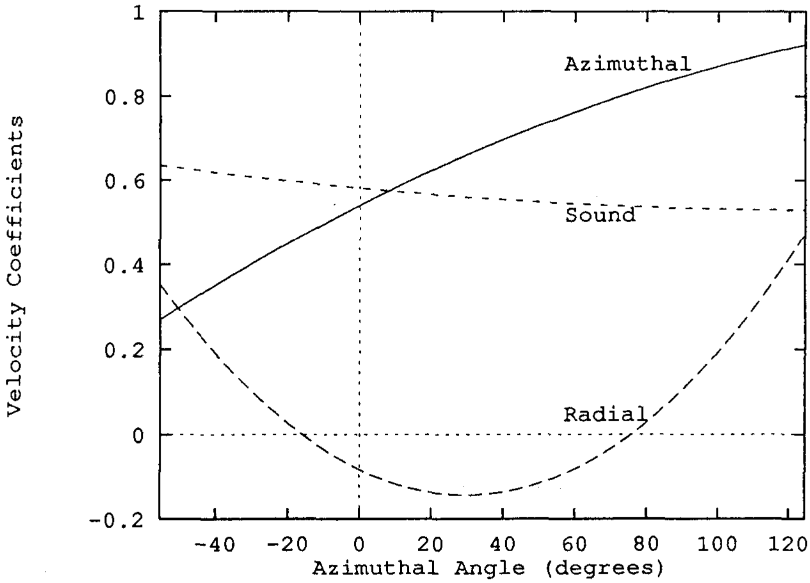

Figure 1. Variations of the velocity coefficients q_i as functions of the spiral coordinate Ψ from the post-shock region (left end) to the pre-shock region (right end). $\Psi = 0$ represents the sonic surface.

present the variation of q_{1-3} in between two shocks as functions of the spiral coordinate $\Psi = \phi + \tan\beta \log(x)$, (sonic surface is at $\Psi = 0$)for $\beta \sim 9^o$ and $q_{2c} = 0.54$. The actual velocity (in units of the velocity of light) is obtained by multiplying these numbers by $x^{-1/2}$, where x is in units of GM/c^2, half of the Schwarzschild radius. The sound speed coefficient (long-dashed) increases from 0.53 to 0.634 at the shock, a jump of about 20% which implies a jump of about 40% of the temperature at the shock front. The azimuthal velocity coefficient (short-dashed) jumps from 0.92 to 0.27 at the shock front. Notice that $q_2 < 1$ always, i.e., the flow is entirely sub-Keplerian. The radial velocity coefficient (solid) goes down from 0.46 to 0.36 at the shock front while becoming negative in some regions, indicating ellipticity of the orbits. Figure 2 compares the line profiles obtained from theory (solid) and observation (dashed) made from various positions of the disk. The mass of the black hole is chosen to be $4 \times 10^9 M_\odot$ and the other parameters are: $i = 42^o$, $v_{th} = 0.0005$ and $q = 2.9$. The dot-dashed curve is the Position 4 observation of [NII] at $\lambda 6584$Å (with H_α blended towards blue widening the base considerably) and the short-dashed curves are the Positions 4, 5, 6 observations of [O III] line at $\lambda 5007$Å. The observations from Positions 1 and 2 roughly match the solid curves drawn for the corresponding positions. Matching using other black-hole mass and inclination angles indicate that

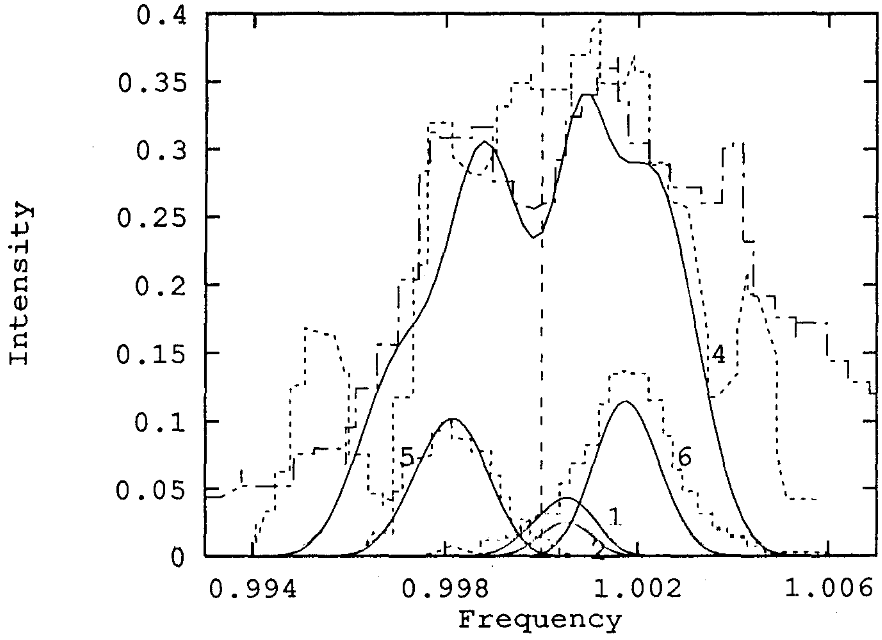

Figure 2. A comparison of the model (solid curves) and observed (dot-dashed for [NII] $\lambda 6584$Å and short-dashed for [O III] $\lambda 5007$Å) line profiles plotted against frequency. The model parameters are: $M = 4 \times 10^9 M_\odot$, $\beta = 9.1^o$, $q_{2c} = 0.54$, $q = 2.9$, $i = 42.0^o$, $v_{th} = 0.0005$. Model curves are marked with Position numbers of HST observation.

the probable mass is $(4 \pm 0.2) \times 10^9 M_\odot$ and the inclination angle is $(42 \pm 2)^o$. The higher mass is due to the fact that our disk is sub-Keplerian.

REFERENCES

Chakrabarti, S.K. 1990, ApJ 362, 406 (Paper 1)

Chakrabarti, S.K. 1995, ApJ (in press)

Chakrabarti, S.K. & Matsuda, T. 1992, ApJ, 390, 639

Chakrabarti, S.K., & Wiita, P.J. 1993, ApJ, 411, 602

Chakrabarti, S.K., & Wiita, P.J. 1994 ApJ, (in press)

Ford, H.C., Harms, R.J., Tsvetanov, Z.I., Hartig, G.F., Dressel, L.L., Kriss, G.A., Davidsen, A.F., Bohlin, R., & Margon, B. 1994, ApJ Letters, (In press)

Harms, R.J., Ford, H.C., Tsvetanov, Z.I., Hartig, G.F., Dressel, L.L., Bohlin, R., Kriss, G.A., Davidsen, A.F., Margon, B. & Kochhar, A. 1994, ApJ Letters, (In press)

Matsuda, T., Inoue, M., Sawada, K., Shima, E., and Wakamatsu, K. 1987, MNRAS, 229, 295

Spruit, H.C. 1987, A & A, 184, 173